MVDC Electric Propulsion Systems for Integrating Waste Heat Recovery Systems in Marine Transport

Juan P. Torreglosa, David Vera Candeas, Diego A. López García, Alejandro Pérez Vallés, José Antonio Hernández-Torres, and Jesus Clavijo-Camacho

***Abstract*— This work proposes a means of reducing maritime transport emissions by combining electric ship propulsion with waste heat recovery systems (WHRSs). This solution was derived from the application of a literature-review-based methodology, the findings of which were formulated as a paradigm consisting of a combination of electric ship propulsion with MVDC networks and WHRSs. This paradigm was then validated through modeling and simulation. Real-time simulations were deployed to evaluate the integration of the heat recovery system, specifically an organic Rankine cycle (ORC), into the MVDC network of the ship. The results of the simulations showed that an appropriate design of the dc network topology and control system is required for the ship to perform correctly under any scenario. It was concluded that replacing the passive rectifiers of the generators with controlled rectifiers improved the voltage profile of the MVDC network. In addition, it was inferred that the design of the global controller is essential for the integration of the heat recovery system.**

***Index Terms*— Marine transportation, marine vehicle control, marine vehicle power systems, marine vehicle propulsion.**

I. Introduction

ONE of the most important challenges currently facing the fields of logistics and world transport is the reduction of emissions from maritime transport. International shipping accounted for ∼2% of global energy-related CO2 emissions in 2020 [1]. As a reference, maritime transport alone exceeded the entire greenhouse gas (GHG) emissions of countries such as Germany and Canada in 2020 [2].

In terms of installed power, heavy-duty diesel engines account for 96% of the energy produced by all ships over 100 gross tons [3], [4]. Because of a lack of alternative propulsion systems with comparable power density, prime costs, and fuel efficiency, it is expected that diesel engines are unlikely to be replaced in the foreseeable future [4]. It is generally accepted that heavy-duty diesel engines have an efficiency of around 50%, with the remaining 50% dissipated as exhaust gas and jacket water. Capturing this waste heat for both electric energy and heat generation would thus result in an improvement in the system efficiency and a reduction of the ship's emissions.

There are a number of works that have reviewed the use of waste heat recovery systems (WHRSs) for ships with heavy-duty diesel engines in order to develop more efficient and cleaner maritime transport [5], [6]. In [5], WHRSs were reviewed from a qualitative and, in some cases, quantitative point of view, including organic Rankine cycles (ORCs). ORCs were found to offer the potential for improving ship efficiency by exploiting waste heat sources from the main and auxiliary engines, with good possibilities in terms of performance, system costs, and dimensions. Alternative WHRSs for marine vessels were qualitatively reviewed in [6]. Although the study concluded that the Kalina cycle achieves higher efficiencies, better savings, and greater emissions reduction than other technologies, including ORCs, these plants had only been tested on land-based sites. However, in both reviews (see [5], [6]), it was stated that ORC systems and prototypes specifically designed for marine applications were currently available on the market. It must be emphasized that the focus of these reviews was a qualitative comparison of different WHRSs with respect to their potential for marine use, rather than exploring how such systems might be integrated with the onboard thermal and electrical power systems. This point is important because the amount of recoverable energy is largely limited by the existing onboard systems, which must be able to absorb it. This point will be discussed in Section II. Another proposal to make marine transport more efficient is the electrification of the propulsion and shipboard power systems [7]. This electrification includes methods such as the integration of energy storage, the tendency toward direct current (dc) power distribution, and the adoption of onboard renewable energy systems, among others.

Section II proposes combining both approaches—WHRSs and electrification—because they are complementary to one another. It will be demonstrated that using electric propulsion increases the capacity to reuse the energy produced by WHRSs.

Manuscript received 25 September 2023; revised 15 December 2023; accepted 8 January 2024. Date of publication 22 January 2024; date of current version 27 December 2024. This work was supported in part by "Programa Operativo FEDER 2014-2020" and "Consejería de Economía, Conocimiento, Empresas y Universidad de la Junta de Andalucía" under Project UHU-202051 and in part by CEI·MAR through the scientific improvement axis of the CEI·MAR 2023 Plan: Research Projects of early-career Ph.D. CEI·MAR 2023 under Project CEI-JD-12 for open access charge: Universidad de Huelva/CBUA. *(Corresponding author: Juan P. Torreglosa.)*

Juan P. Torreglosa, Alejandro Pérez Vallés, José Antonio Hernández-Torres, and Jesus Clavijo-Camacho are with the Department of Electrical Engineering, University of Huelva, 21004 Huelva, Spain (e-mail: juan.perez@die.uhu.es).

David Vera Candeas is with the Department of Electrical Engineering, University of Jaén, 23700 Linares, Spain.

Diego A. López García is with the Department of Electronic Engineering, Computer Systems and Automating, University of Huelva, 21004 Huelva, Spain.

Digital Object Identifier 10.1109/TTE.2024.3356655

The main objective of this work was to find the most appropriate way to integrate WHRSs (specifically ORCs or Kalina cycles) with shipboard power systems and to validate it. The procedure followed was as follows. First, a literature review was carried out to establish the best paradigm for the integration of WHRS with shipboard power systems. The methodology applied in this stage involved going through the literature in a logical order, starting with the selection of the best WHRS for ships. Following this, in light of the results of this review, the search was broadened to identify all feasible solutions. Then, subject to a set of predetermined goals, each potential solution was evaluated and those failing to satisfy those goals were gradually excluded until only one remained. This was chosen as the best option, and the process was repeated until the paradigm was defined. Second, once the paradigm had been defined, it was subjected to a validation methodology based on modeling and simulation. This involved the creation of a simulation model that met the specifications of the paradigm. The model took the form of an electrical model developed to enable the integration of the WHRS with the shipboard power system to be studied in terms of identifying the chief technical challenges and finding the optimal solutions.

The main contributions of this article are the following.

1) The selection of the best paradigm for the integration of WHRS in shipboard power systems via a comprehensive literature review.
2) The resulting proposal, a combination of an ORC system with dc electric propulsion, is a novel solution that has not been studied in previous literature.
3) The research involved the development of a model of a pulsewidth modulation (PWM) rectifier based on controlled average-value power converters which is able to run real-time simulations.
4) The model of an electric ship with a medium-voltage direct-current (MVDC) network available in [8] has been updated, replacing its passive rectifiers with the controllable rectifiers described in contribution three above.
5) Real-time simulations were deployed to evaluate the proposed paradigm for the integration of WHRSs in shipboard power systems.

Regarding the validation of the proposed paradigm, hardware-in-the-loop (HIL) testing is a simulation technique that is commonly used in the early design stages of shipboard power systems to demonstrate that the proposed technology can be applied to real systems [9]. HIL testing requires models that can run in real time. Recent studies tested control strategies using real-time verification for electric propulsion ships [10], [11], [12], [13], [14]. Hou et al. published [10], in which two model predictive controller (MPC)-based energy management (EM) strategies (control with prefiltering and coordinated control) for dc all-electric ships were compared in terms of addressing power tracking and energy saving, and optimizing the use of a hybrid energy storage system composed of batteries and ultracapacitors. Real-time simulations were carried out to conduct the comparison. The same year, some of the members of the team that published this work presented [11]. In this instance, the EM strategy applied to the same electric ship powerdrive was based on an MPC whose objective was to mitigate load fluctuations and minimize losses in the storage system. The proposed strategy was tested in a laboratory test bed whose power electronic converters were controlled in real time by a Speedgoat target machine used as microcontroller (i.e., using an HIL testing approach). Hou et al. [11] proposed in [12] a new solution to mitigate load fluctuations from the shipboard network: combining battery and flywheel as a hybrid energy storage system. This solution required an MPC to be implemented in real time. This solution was validated against previous battery-ultracapacitor-based hybrid energy storage system through real-time simulations. A real-time simulation framework of a dc shipboard microgrid, including models of propellers, prime movers, electrical machines, battery energy storage systems, power converters, and regulators, was developed in [13]. The results of real-time simulations showed that several control schemes could be implemented, to test system performance under different conditions, and to verify operational constraints during the expected ship missions. The proposed architecture was realized to allow HIL configurations for experimental validation in future works. Nunez Forestieri and Farasat [14] also proposed a solution to mitigate load fluctuations in MVDC ships based on hybrid energy storage systems, as was proposed in [10], [11], and [12]. In this case, the proposed solution was developed based on the premise that the dimensioning of the storage system and the design of the EM strategy were linked and mutually affected each other. Thus, sizing and EM strategy were jointly optimized by using a deep reinforcement learning-based method. Implementation feasibility and adaptability to various ship propulsion power profiles was confirmed through real-time simulations. In a similar fashion to these studies, the work presented in this article was validated through real-time simulations, although unlike those they were utilized to verify both the control strategy and the integration of a WHRS.

The structure of this article is as follows. Following this Section I, Section II describes the selection of the most suitable WHRS in combination with the topology of the ship propulsion system via a review of the existing literature in order to define the proposed paradigm. Section III then details the characterization of the components of the paradigm obtained from recent works. Section IV shows the results of the validation of the proposed paradigm. This is used as a test bench to analyze different scenarios resulting from the integration of the WHRS with the shipboard network. These scenarios are studied by means of real-time simulations. Discussion of the results is presented in Section V, highlighting both the limitations and the opportunities of the models and real-time simulations developed in the work and also suggesting future areas to be developed. Finally, the conclusions drawn from this work are presented in Section VI.

II. Defining a Paradigm for WHRS Integration in Ships From a Literature Review

In this section, drawing on an extensive review of the existing literature, a paradigm is developed to identify the

ships most suitable for the integration of WHRS. The applied methodology consists of following a logical sequence in which potential solutions are successively excluded according to a set of predefined objectives until one solution remains that meets all the objectives and is regarded as the finest choice. The choice of the WHRS that best matches the characteristics of the exhaust gas from shipboard diesel engines should therefore be made first.

A. WHRS Selection for Ships

Under nominal conditions, the temperature range of the exhaust gas of heavy-duty diesel engines varies according to the ambient and load conditions, from 325 °C to 345 °C for two-stroke engines, and from 400 °C to 500 °C for four-stroke engines [15]. In order to work optimally, WHRSs need to be capable of adjusting and adapting to both the variability of operating conditions (slow transit, rapid transit, maneuvering, ocean towing, anchor handling, and so on), and the ambient conditions, such as water temperature (dependent on the location and season).

A review of different WHRSs was conducted for marine vessels in [6]. Although it concluded that the Kalina cycle achieves higher efficiencies, better savings, and greater reductions in emissions than other technologies such as the Rankine cycle or ORC, these plants have only been tested on land-based sites. However, in the case of ORC, there are systems specifically designed for marine applications currently available on the market (e.g., the first onboard plant of this type developed by OPCON Marine [16]). An ORC is a modified form of the Rankine cycle, which uses other organic fluids instead of water/steam as the working fluid of the system. It has the same basic components as the Rankine cycle, producing mechanical work in a turbine that drives a generator to produce electricity. The Kalina cycle is also essentially a modified Rankine cycle, in this case utilizing the mixture of two different compounds as the working fluid (water and ammonia). It also produces mechanical power in a turbine driving a generator to produce electricity. However, due to their simplicity, ORC-based systems have received more attention for marine applications.

Once the selection of best-performing ORC for large tonnage ships is made, the next step is to assess the available propulsion systems for ships to determine which is most suitable for integration with the ORC.

B. Integration of ORC-WHRS in the Electric Power System

As mentioned above, the main WHRSs for marine applications (Kalina cycles and various Rankine cycles) transform part of the exhaust gas energy into electrical energy via turbines and generators. This electricity must be reused in the electrical power system of the ship to improve the system efficiency. The integration of the generator of the WHRS in the ship's electrical network requires power management. Although the focus of this work is on the ORC, the solution proposed here could also be integrated with other types of WHRSs, giving the thermal element of these systems complete operational freedom.

However, not all ship propulsion systems are suitable for the recovery of energy in the form of electricity.

According to their propulsion system, ships can be classified as mechanical or electrical [17]. In mechanical propulsion systems, the propulsors of the ship are driven by diesel engines either directly or through a gearbox. Additional diesel generators feed a separate alternating current (ac) network to distribute electric power to the ship's auxiliary loads. In electrical propulsion systems, multiple diesel generator sets feed an electrical bus to which both the motor drives (in charge of the propulsion) and the auxiliary loads are connected.

Regarding the integration of ORC-WHRS, it must be highlighted that, in terms of power rates, the propulsion of the ship is the main power demand of the system. In mechanical propulsion systems, the electricity generated by the WHRS would be limited to use in feeding the auxiliary loads and would result in overcharging the electrical network. In electrical propulsion systems, this problem does not arise since all the electricity generated by the WHRS is injected into the common distribution system that feeds both the propulsion and auxiliary loads. Furthermore, as the propulsion power demand increases, so the diesel generator output increases and, likewise, the electricity generated by the WHRS. Thus, the recovery power is coupled with the propulsion load power, avoiding any overcharge of the electrical network. In conclusion, electrical propulsion is the most suitable candidate for integration with WHRS.

Apart from this advantage, there are other factors, as noted in [18] and [19], motivating fleets worldwide to move toward electric propulsion, primarily connected with the continuing progress being made in power electronics. Eliminating the mechanical drive makes it possible to install the components of the ship in locations that offer the most efficient packaging and weight distribution. The overall efficiency of electric propulsion is considerably higher than that of an equivalent mechanical propulsion design, particularly at low speeds [19]. In addition, electrical propulsion reduces vibration, increases the flexibility of operation (e.g., in the case of damage), increases reliability by making it possible to transmit power using redundant cables (redundant shafts are not possible), reduces maintenance tasks, allows the integration of new energy conversion devices (e.g., fuel cells and batteries), and is mandatory for high-power mission systems in warships (e.g., laser weapons and high-power radars) among others [18], [19].

Nevertheless, when choosing the best electric propulsion system for ORC integration, there are two subcategories of electric propulsion to consider, ac and dc, each with its benefits and drawbacks.

C. Electric Propulsion: AC Versus DC

Although until now ac power has been the preferred system in marine vessels, advances in modern power electronics and other technology have prompted discussion about the use of dc or ac distribution. Skjong et al. [20] collated key points from the literature on whether to use ac or dc. Below is a summary of the chief considerations regarding integration of WHRS into the electrical grid.

1) In dc systems, since frequency control is not a concern, the prime movers can be run at optimized speeds [20]

2) In dc systems, phase matching is not needed [20]. Therefore, dc systems ease the paralleled operation between the main diesel generators and the generator of the ORC system (whose generator speed depends on the operation point of the ORC)

3) Other advantages [20]: the weight of cables may decrease for a given power level for dc versus ac systems; in dc systems, medium- or high-frequency transformers (dc–ac–dc electronic transformers) can be used, resulting in a smaller footprint; and in dc systems, high-speed gas turbines can be used in conjunction with high-speed generators, without the need for reduction gears for frequency control, thus reducing weight and space. These advantages are supported by other studies [7], [21], [22] that point to a reduction of space and weight in the electrical components of the network by up to 30% for dc systems in comparison with their ac counterparts.

The adoption of dc technology for electrical propulsion through MVDC power systems was studied from the point of view of power electronics in [23]. This article identifies the marine sector as a leading sector for the study and experimentation of MVDC and notes that one of the challenges for improving performance in ships' power systems is the shift from MVAC to MVDC.

The interconnection of the power sources and system loads in an MVDC network requires power converters. It results in the multiterminal network defined next.

D. Voltage Source Converter-Based Multiterminal MVDC Network

The resulting electrical network is a multiterminal (MT) dc network in which the terminals correspond to the different generators and loads. MT dc systems have become a realistic solution for domestic and international power transmission at high voltage (HV) levels, as the number of systems in operation and projects planned show [24]. The adaptability of voltage source converters (VSCs) makes it possible to adapt the well-known MT HVDC systems to a lower power level, i.e., to medium voltage (MV) resulting in MT MVDC systems. The voltages of these VSCs can be increased by connecting groups of IGBT switches in series [25].

With regard to the generators, the VSCs operate as force-commutated PWM rectifiers. In comparison to line-commutated converters based on thyristors (whose turn-off conditions are determined by the voltages of the ac supply line), the use of IGBTs (with gate turn-off capability) allows full control of the converter, replacing the phase control of output voltage by PWM. Thus, the voltage source rectifier operates by keeping the dc link voltage at a desired reference value, using a feedback control loop where the dc link voltage is measured and compared with a reference voltage [26].

Regarding the propulsion loads, the well-known VSCs are commonly applied for medium- and high-power traction and industrial high-power drives due to their capacity for four-quadrant operation and reversibility [25].

Taking everything into account, the resulting VSC-MT MVDC network is well suited to the integration of the ORC-WHRS in ships in terms of adaptability, flexibility, and technological maturity. However, this integration depends on proper control of this VSC-MT MVDC network. According to [24], the challenge for the control of this kind of grid is the tradeoff between voltage regulation and power sharing. It can be achieved under necessary constraints on the dc bus voltages and power sharing ratio.

E. Control of the VSC-MT MVDC Network

The proposed VSC-MT MVDC network requires an adequate control system to keep the dc voltage of all the buses within permissible limits and ensure precise control of the power sharing. In [24], a theoretical framework for the control of VSC-MTDC systems was developed and a novel distributed control was proposed for them. The following control premise was stated: since the dc voltage control and power sharing are objectives that oppose each other, a tradeoff between the two objectives must be found. The approach to solving this control problem was through a two-layer control framework, as proposed in [27]. The general idea is to use a droop control in the primary level in charge of dc voltage regulation at the dc terminals, control of active and reactive power at the point of common coupling (PCC), and maintaining the PCC's ac voltage at the specified setpoint. Then, the secondary level uses a control that modifies the droop characteristics of the primary controllers enabling both control objectives (voltage regulation and power sharing). The control strategies that can be implemented in the second layer can be categorized as centralized control [27] and decentralized control [24]. The difference between them is that the centralized control uses a single control unit that is in communication with all the buses of the system, while the decentralized control uses one control unit for each bus with no communication between them. In the case of ship networks, their size is limited to the ship dimensions (the distances on board are short, typically under 1 km [19], [28]) so it does not make sense to consider decentralized control in the second layer.

III. Modeling of the Components of the Paradigm for WHRS Integration in Ships

The above section defined the ship's network as a VSC-MT MVDC network with a centralized two-layer control. This section now describes the characteristics required of the components making up this network. Sources for defining these characteristics include recent works that have studied MVDC networks for ships from different approaches [28], [29], [30], [31], [32], [33] and published standards and guidelines [34], [35], [36], [37].

The model provided in [33] has been considered as the template for modeling the proposed paradigm because its architecture (a ring topology with two zones) can be seen as a representative simplification of the notional MVDC system described in the IEEE Standard 1709-2018 for a high-performance ship [34] (a ring topology with five zones). Although a simplification, it is sufficiently complex to analyze the impact of the integration of the ORC-WHRS. The power rating of this model fits with certain types of ship using

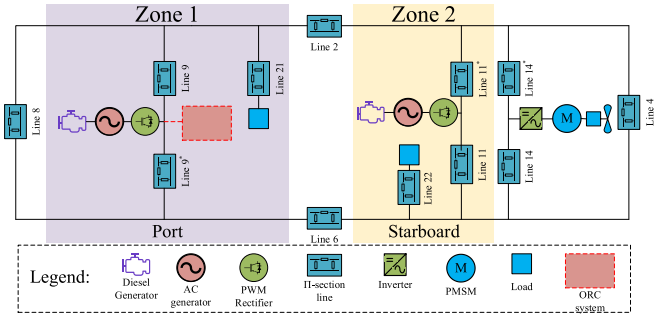

Fig. 1. Topology of the two-zone shipboard MVDC network.

TABLE I
GENERAL FEATURES OF THE PROPOSED MODEL

Feature	
Generation power	2x36 MVA
Distribution voltage	1.5 kV
Electrical generators	2xSalient-pole synchronous machine
Generator prime movers	Diesel engine
Auxiliary loads	2x1 MW
Propulsion load	36 MW
ORC net power	18MW
ORC power generation system	Salient-pole synchronous machine + diode rectifier

electric propulsion [38], including field support vessels, cruise vessels, ferries, and oil/LNG tankers. Most of these vessels are typically propellers driven, powered by diesel engines or, less typically, gas turbine engines, combined in both cases with electric propulsion.

The topology of the model proposed is shown in Fig. 1. The MVDC network is composed of two zones, where Zone 1 contains one generator system and one load system and Zone 2 contains one generator system, one load system, and one propulsion system. This power system diagram is a simplified version of what would actually be used in real ships. In real ships, each one of the generation systems shown in the diagram (including the ORC system) would be split into parts by using different electrical buses and bus ties in order to provide redundancy. Nevertheless, what Zones 1 and 2 do represent is the practice of installing two power systems, usually both port and starboard. The general features of the paradigm are outlined in Table I. In terms of power and voltage ratings, it could represent the power scheme of a shuttle tanker with single screw propulsion [38], whose distribution voltage of 11 kV–60 Hz would be replaced by a 12-kV dc network (with the necessary inclusion of proper power converters).

The lines are represented by π-section models, the parameters of which are given in Table II. As stated in [28], these models offer fair accuracy given the short lengths of the cables. In addition, since the lines can be considered short, line

TABLE II
PARAMETERS OF THE π-SECTION LINES

Line #	Resistance (mΩ)	Inductance (μH)
2	0.21	3.47
4	0.21	3.47
6	0.21	3.47
8	0.30	4.91
9	0.16	2.63
9*	0.16	2.63
11	0.32	5.32
11*	0.32	5.32
14	0.21	3.42
14*	0.21	3.42
21	0.26	4.30
22	0.28	4.73

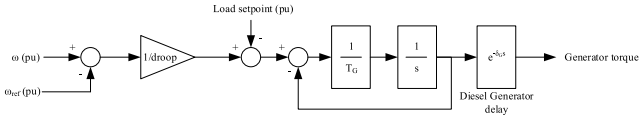

Fig. 2. Block diagram of the diesel engine governor model.

capacitance of the π-section model can be neglected because of the small leakage current.

The generator systems were modeled using three components: a diesel generator, a rectifier, and an output filter consisting of an *RC* low-pass filter. In turn, the diesel generator model was composed of a salient-pole synchronous machine, a diesel engine governor, and the exciter module. The synchronous machine and the exciter were modeled using the corresponding blocks from the Simscape Electrical[1] library, the values of which are shown in Table III. In the original model in [33], the prime movers were gas turbines. In this work, they have been replaced by diesel engines, as these are more common in electric propulsion ships [38]. The model proposed for the diesel engine governor was built following the block diagram in Fig. 2. This represents the action of the throttle actuator of the diesel engine. It compares the reference speed and the measured speed for the synchronous motor and generates the diesel engine mechanical power that is related to the throttle operation point. The reference speed and the load setpoint were set at 1 and 0.5, respectively. Regarding the rectifier, the original model in [33] used an ideal power converter that held the dc voltage to a reference and drew unity power factor on the ac side. This ideal power converter model has been replaced by an averaged model of a force-commutated PWM rectifier, which is described fully in Section III-A.

The load systems were modeled as resistive loads directly connected to the dc bus representing the auxiliary loads of the ship. Each load system was rated for 1 MW.

[1]Trademarked.

TABLE III
PARAMETERS OF THE GENERATOR SYSTEMS

Parameter	Value
Synchronous Machine Model Parameters	
Rated MVA of the Machine	36 MVA
Number of q-axis rotor windings	1
Rated RMS line-to-line voltage	13.8 kV
Base frequency	60 Hz
Inertia Constant, H	4 s
Synchronous Mechanical Damping, D	0.04 pu
Stator Leakage Reactance, X_a	0.08 pu
D-axis Unsaturated Reactance, X_d	1.352 pu
D-axis Unsaturated Transient Reactance, $X_{d'}$	0.296 pu
D-axis Unsaturated Sub-Transient Reactance, $X_{d''}$	0.148 pu
Q-axis Unsaturated Reactance, X_q	0.836 pu
Q-axis Unsaturated Sub-Transient Reactance, $X_{q''}$	0.122 pu
Stator Resistance, R_a	0.006 pu
D-axis Unsaturated Sub-Transient Open Time Constant, $T_{do'}$	4 s
D-axis Unsaturated Sub-Transient Open Time Constant, $T_{do''}$	0.03 s
Q-axis Unsaturated Sub-Transient Open Time Constant, $T_{qo'}$	0.2 s
Diesel Engine Parameters	
Percentage Droop, *droop*	0.05 pu
Governor Time Constant, T_G	0.2 s
Diesel Generator Time Delay, δ_G	0.3 s
Load setpoint	1 pu
AC1A Exciter Parameters	
Filter Time Constant, T_r	0.001 s
Voltage Regulator gain, K_a	80 pu
Voltage Regulator Time Constant, T_a	0.2 s
Voltage Regulator Internal Limits, [V_{Amin} , V_{Amax}]	[-15,15] pu
Voltage Regulator Output Limits, [V_{Rmin} , V_{Rmax}]	[-14.99,14.99] pu
Damping Filter Gain, K_f	0.03 pu
Damping Filter Time Constant, T_f	1.49 s
Exciter Gain, K_e	1 pu
Exciter Time Constant, T_e	0.2 s
Exciter Alternator Voltage Values, V_{e1} and V_{e2}	5 and 4 pu
Exciter Saturation Function Values	[0.4 0.5] pu
Demagnetizing Factor, K_d	0.4 pu
Rectifier Loading Factor, K_c	1 pu

TABLE III
(Continued.) PARAMETERS OF THE GENERATOR SYSTEMS

ORC Model Parameters	
Turbine Inlet Temperature	260 ºC
Turbine Inlet Pressure	30 bar
Condensing Temperature	18.3 ºC
Mass Flow Rate at 100% load	4.38 kg/s
Pump Isentropic Efficiency	75%
Turbine Isentropic Efficiency	85%
ORC Generator Electric Efficiency	94%

The propulsion system was modeled as a permanent magnet synchronous motor (PMSM) connected to the MVDC through an average-value VSC using the corresponding blocks from the Simscape Electrical library. A field-oriented control (FOC) was implemented to control the VSC of the propulsion system. The power losses of the VSC were simplified to a reasonable fixed loss of 5% of the converter rated power [39].

The ORC generation system was composed of a gas turbine, a permanent magnet synchronous generator (PMSG), a passive rectifier, and an *RC* filter. The gas turbine acted as prime mover providing the mechanical torque to the generator. Radial turbines are the first choice for ORC-WHRS applications with electric power outputs from tens of kilowatts to several megawatts [32]. In order to simplify the mechanical configuration of the system and to reduce costs, it is preferable to have the turbine directly connected to the generator. For this reason, the generator determines the speed of the expander according to the number of poles it has and grid frequency [32]. Regarding the electrical generator, a PMSG is a common choice owing to its higher efficiency, robustness, zero excitation losses, reliability, and lower weight/size in comparison to other types of generators. The PMSG must be connected to the dc bus through an ac-to-dc converter. The simplest solution is a three-phase diode-bridge rectifier with the dc voltage ripple filtered by a capacitive filter. Although it has a simple construction and high conversion efficiency, this architecture cannot actively regulate the dc-bus voltage [33]. However, if the output of this rectifier is connected to a dc bus whose voltage is regulated, as is the case here, and as long as the back EMF magnitude of the generator is higher than the dc bus voltage, then the generator/rectifier system can be modeled as an ideal current source [34]. Under these conditions, the generator/rectifier system shows stability against rotational speed disturbances: if the disturbance is positive, the torque will increase and brake the rotor, if the disturbance is negative, the torque will decrease, allowing the rotor to regain speed [34]. Taking everything into account, this system can be modeled as an ideal current source connected in parallel with the generator system of Zone 1. The power of the current source is represented by a function dependent on the temperature of the exhaust gases of the diesel engines. This

model can be used to represent other WHRSs with generators, e.g., a Kalina cycle, making the appropriate adaptions to the power functions. As mentioned above, the power system diagram in Fig. 1 is a simplified version of what would really be used in actual ships. In a real shuttle tanker, each diesel engine in the figure would be split into two 18-MVA (14.4 MW) diesel generators, the characteristics of which correspond to those of a four-stroke Wärtsilä 12V46F diesel engine driving a generator. Homologically, the ORC system represented in Fig. 1 would be split into four ORC systems, one for each real diesel genset; 18 MW of ORC net power displayed in Table I is the sum of four 4.5-MW ORC systems. The function for the power generation of the ORC system was developed from the datasheet of the Wärtsilä 12V46F engine [40], which provided the exhaust gas temperature for four different loads (50%, 75%, 85%, and 100%). Based on the R1233zd organic fluid characteristics [41] and the performance of the Wärtsilä 12V46F diesel engine, a model of an ORC was created in Cycle-Tempo[1] to calculate the power of the generator when driven by the turbine according to the four temperatures of the exhaust gases from the diesel engine provided by the datasheet. The resulting function, see the following equation, corresponds to the interpolation of the four operating points:

$$\mathrm{P_{ORC}} = -0.2286\mathrm{P_{DE}^3} + 0.9943\mathrm{P_{DE}^2} - 0.8514\mathrm{P_{DE}} + 0.4057 \tag{1}$$

where P_{ORC} and P_{DE} are the power in per-unit (pu) of the ORC system and the pu load of the diesel engines (defined as the percentage of the maximum power of the diesel engines), respectively, considering the base power of the pu system the total power of the diesel engines. Note that this equation's application range starts at a load of 50%, and that at lower load values in this work, the ORC generation is regarded as null. The parameters of the ORC model are given in Table III.

In summary, the paradigm proposed in this work for the study of VSC-MT MVDC networks is a modified version of the model proposed in [33]. Like that model, it was built using the Simscape Electrical library but replaced the ideal passive rectifiers with PWM rectifiers, substituted the gas turbines for diesel engines, and added an ORC system to the network. These modifications resulted in a more complex model without affecting its capacity to run simulations in real time.

A. Proposed Model of the Force-Commutated PWM Rectifiers

The force-commutated PWM rectifiers connected to the generators are voltage source rectifiers that operate by keeping the dc link voltage at a desired reference value, using a feedback control loop, as shown in Fig. 3(a). To accomplish this task, the dc link voltage is measured and compared with a reference V_{ref}. The error signal generated from this comparison is used to create a PWM pattern for each phase whose fundamental voltage is a voltage with the same frequency as the ac voltage. When the rectifier is controlled in this way, it ensures that the six diodes are polarized negatively at all values of instantaneous ac voltage supply, and therefore, it operates as a boost converter whose output dc voltage can only be stepped up over the dc output voltage that would result from a diode-bridge rectifier [42].

In this study, a controlled average-value power converter was developed to reproduce the behavior of these rectifiers. The model, shown in Fig. 3(b), contains a controlled current source for each phase on the ac side and a controller voltage source on the dc side, while the duty cycle is the control input to convert the electrical energy between each side of the converter. It thus converts instantaneous three-phase ac voltages to dc voltage and dc power demand to three-phase ac power demand. In addition to this, a fictional dc bus was incorporated, the voltage of which is that which would result from a diode-bridge rectifier. The equations that define the model are described as follows.

The dc output voltage that would result from a diode-bridge rectifier V_g is calculated as

$$V_{\mathrm{RMS}} = \frac{\sqrt{(v_a - v_b)^2 + (v_b - v_c)^2 + (v_c - v_a)^2}}{3} \tag{2}$$

$$V_g = 3\frac{\sqrt{2}}{\pi} V_{\mathrm{RMS}} \tag{3}$$

where v_a, v_b, and v_c are the respective ac phase voltages, V_{RMS} is the rms ac line-to-line voltage, and V_g is the dc voltage between the positive and negative terminals of a diode-bridge rectifier.

The relationship between the dc voltages at the input and output of the boost converter shown in Fig. 3(b) is

$$\frac{V_{\mathrm{dc}}}{V_g} = \frac{1}{1 - D_c} \tag{4}$$

where D_c is the duty cycle generated by the control loop to control the dc output voltage V_{dc} of the rectifier.

Then, since the converter is considered to be ideal (i.e., the three-phase ac power at its input is equal to the dc power at its output)

$$P_{\mathrm{ac}} = P_{\mathrm{dc}} = I_{\mathrm{dc}} V_{\mathrm{dc}} \tag{5}$$

$$R_{\mathrm{ac}} = \frac{V_{\mathrm{RMS}}^2}{P_{\mathrm{ac}}} \tag{6}$$

$$v_{\mathrm{ref}} = \frac{(v_a + v_b + v_c)}{3} \tag{7}$$

$$\begin{bmatrix} i_a & i_b & i_c \end{bmatrix} = \frac{\begin{bmatrix} v_a & v_b & v_c \end{bmatrix} - v_{\mathrm{ref}}}{R_{\mathrm{ac}}} \tag{8}$$

where P_{dc} is the power output on the dc side, P_{ac} is the power input on the ac side, I_{dc} is the current output on the dc side, R_{ac} is the per-phase series resistance in an equivalent wye-connected load, i_a, i_b, and i_c are the phase currents on the ac side, and V_{ref} is the dc offset on the ac side (in a balanced power system with no dc bias, it is 0 V).

With dynamics appropriate for real-time simulations, the resulting model represents an implementation of an ideal controlled average-value PWM rectifier with a good fidelity/complexity ratio.

B. Centralized Control for the PWM Rectifiers

Section II-E described the challenge facing a centralized secondary control for an MVDC network with controlled

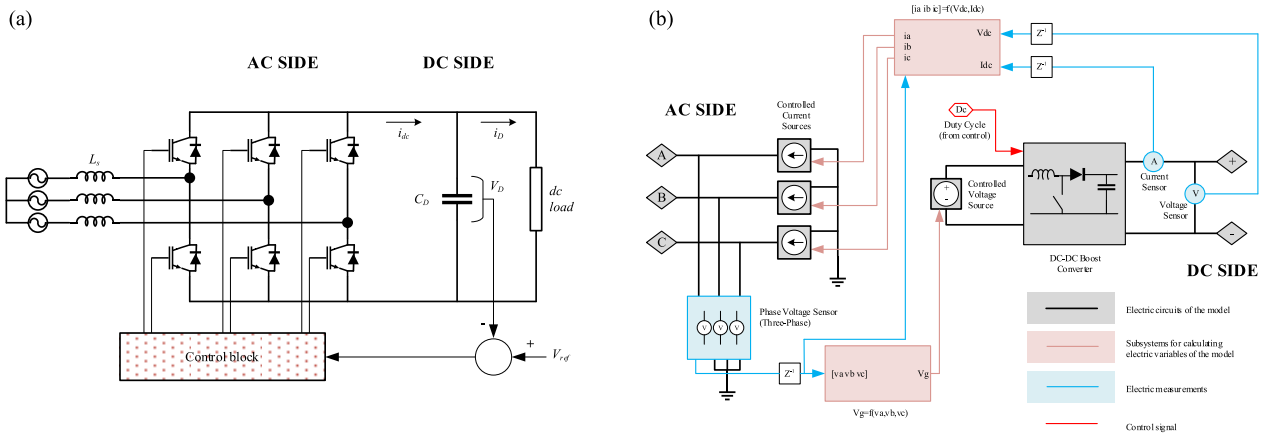

Fig. 3. PWM rectifier modeling. (a) Electrical scheme and control and (b) block diagram of the proposed model for the PWM rectifier.

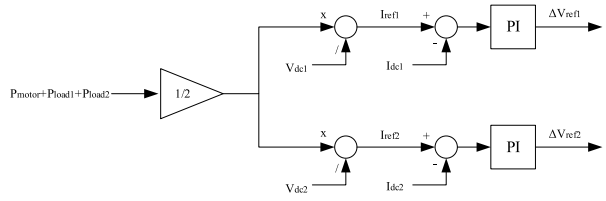

Fig. 4. Block diagram of the centralized controller for generating the voltage references for the control loops in the PWM rectifiers of the generators.

power converters, namely, keeping the dc voltage of all the buses within permissible limits and ensuring that power sharing is controlled with sufficient precision. Although the development of centralized controllers is not within the scope of this work, a simple centralized controller was developed to study the effects of integrating the ORC-WHRS into the MVDC network.

The objective of the centralized controller is to ensure equal power sharing between the two generators in the system. A diagram of this control is shown in Fig. 4. It estimates the reference power to be generated by each PWM rectifier as half of the total power demanded by the network. Once the reference powers have been estimated, a reference output current for each rectifier is calculated dividing the reference power by the measured output voltage of the rectifier. Then, a PI controller compares this reference current to the measured current to generate a reference voltage variation, ΔV_{ref}. ΔV_{ref} is then added to the reference voltage, V_{ref}, of each rectifier control loop. If the reference current is lower than the measured current, $\Delta V_{\text{ref}}$is negative, so the reference voltage controlling the rectifier decreases in order to increase the output current. If the reference current is higher than the measured current, ΔV_{ref} is positive so the reference voltage controlling the rectifier increases in order to decrease the output current.

IV. Results

This section evaluates the proposed solution for reducing the fuel consumption of marine transport by combining electric propulsion and WHRS. The model described in Section III was used as a test bench to analyze different scenarios resulting from the integration of the ORC in the shipboard network. These scenarios were studied in simulations deployed and tested on a speedgoat performance real-time target machine with four Intel Core i7 4.2-GHz processors, as shown in Fig. 5. The scenarios are summarized in Table IV and described in greater detail next.

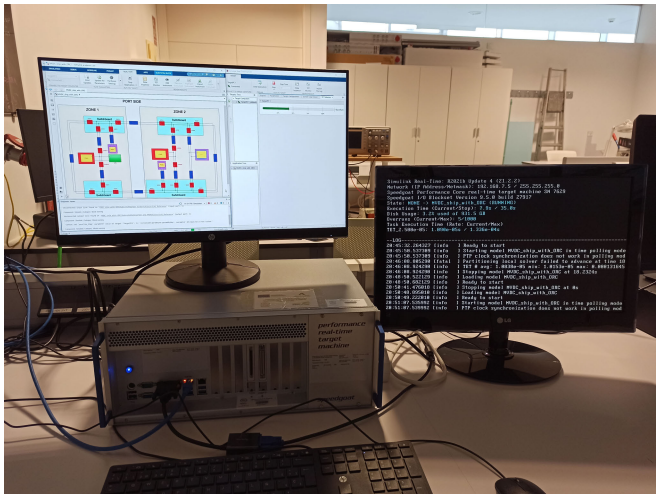

Fig. 5. Speedgoat performance real-time target machine executing a real-time simulation of the proposed scenarios.

In order to evaluate the performance of the integrated ORC, three different case studies were simulated. The first replicated the original model [33], which used ideal diode rectifiers for the generators and served as a template for the proposed paradigm. The power sharing between the generators was enabled through voltage droop, set to the same values so as to provide the same power. The second and the third case studies corresponded to simulations using the model based on the proposed paradigm. In the second, each of the generators' PWM rectifiers was controlled to keep their buses' dc voltage at a fixed reference value of 12 kV. In the third case, the reference values for the control loops of each PWM rectifier were sent by the centralized control described in Section III-B. Each case study was simulated with and without the ORC system.

TABLE IV
CASE STUDIES AND SCENARIOS

Case studies		Scenarios
I. Ideal diode rectifiers with fixed power sharing between generators	*w/o ORC*	*s.s.r.m.*
		t.o.p.
	w/ ORC	*s.s.r.m.*
		t.o.p.
II. PWM rectifiers controlled to keep the voltage of their buses at a fixed reference value	*w/o ORC*	*s.s.r.m.*
		t.o.p.
	w/ ORC	*s.s.r.m.*
		t.o.p.
III. PWM rectifiers operating under a centralized control modifying the reference voltages of each bus	*w/o ORC*	*s.s.r.m.*
		t.o.p.
	w/ ORC	*s.s.r.m.*
		t.o.p.

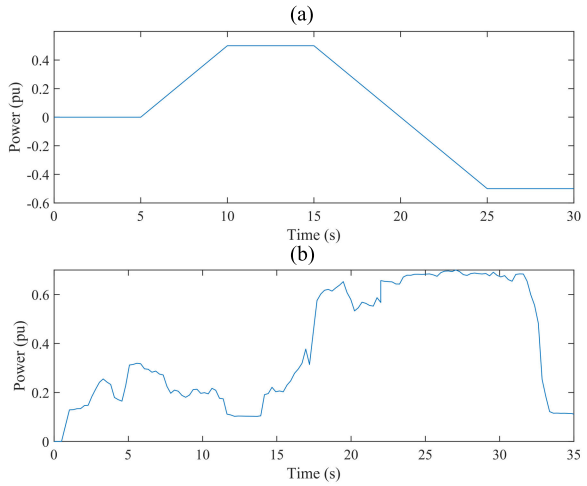

Fig. 6. Ship profiles for the case studies. (a) Shaft speed reversion maneuver (s.s.r.m.). (b) Typical operational profile (t.o.p.).

In those case studies featuring the ORC system, its power was calculated as a function of the power of the generator systems using (1). The ORC system worked as a current source dependent on the operation of the generators, which involved a disturbance to the network.

Finally, for each case study, the following scenarios were proposed: a shaft speed reversion maneuver (s.s.r.m.) and a typical operational profile (t.o.p.). The shaft speed reversion maneuver represents a critical scenario in emergencies when the ship must be capable of reversing its shaft speed in order to stop its advance as quickly as possible. As the name suggests, the typical operational profile represents the range of operations typically required of a cruise ship, as described in [43], such as sailing, stops in ports, departures, and the like. In this work, a portion of this typical operational profile was resized for a simulation length of 35 s, sufficient time to analyze the system's dynamic response. Since the transitions were executed in considerably less time than the original, the profile became even more challenging. The ship speed versus time profiles for the two scenarios are shown in Fig. 6.

The results of these simulations are described in the subsections next.

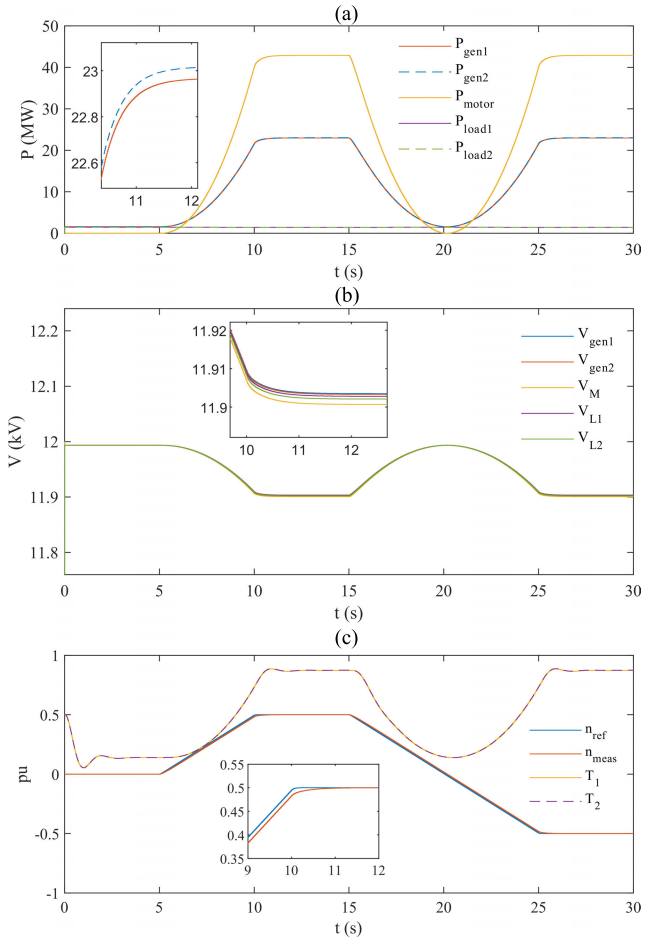

Fig. 7. Case study I, s.s.r.m. scenario w/o ORC. (a) Power, (b) voltage, and (c) propulsion speed and torque of the generators.

A. Case Study I

This case study corresponds to the system using ideal diode rectifiers for the generators. Power sharing between the generators was enabled through voltage droop, with the same droop values being set to provide equal power.

Fig. 7 shows the system operation without the ORC during an s.s.r.m. The powers of the different components are shown in Fig. 7(a). The main power demand is from the ship's propulsion, which increases from 0 to around 42 MW in 5 s to comply with the shaft speed command (0.5 pu). Following this, the reversion maneuver is carried out by transitioning from a shaft speed command of 0.5 to one of -0.5, a procedure which takes 10 s. This results in a predictable fall and rise in the required power for the propulsion. The power is evenly distributed across the generators during this maneuver [see Fig. 7(a)]. Fig. 7(b) shows the voltage of the buses where the generators, propulsion system, and loads are connected. It can be observed that the voltage drop in the different buses increases when the demand for propulsion power increases. The maximum voltage drop, 1.27%, corresponds to the bus where the propulsion system is connected. The remainder of the buses present similar voltage drops, all within the limits imposed by the various standards governing electric ships with dc distribution networks: "steady-state (continuous)

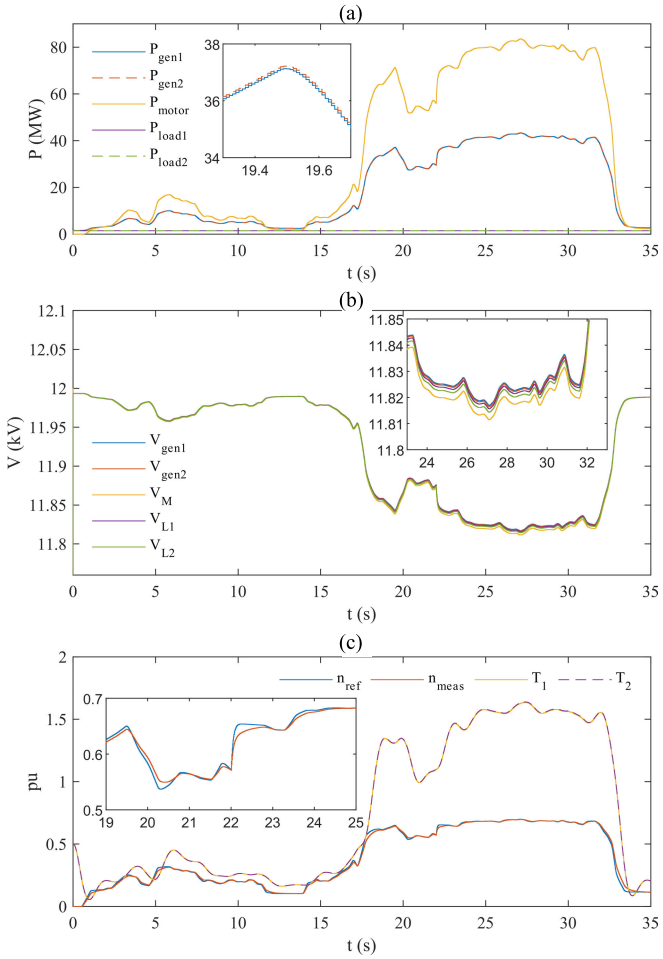

Fig. 8. Case study I, t.o.p. scenario w/o ORC. (a) Power, (b) voltage, and (c) propulsion speed and torque of the generators.

dc voltage tolerances limits should be ±10%" [34]; "for all distribution circuits, unless stated otherwise, the combined maximum voltage drop from the ships service switchboard to any point in the system should not exceed 5%" [44]. Finally, Fig. 7(c) shows that the propulsion system correctly followed the shaft speed command with a delay of less than a second. In addition, it shows the mechanical torque applied to the shafts of the generators in per unit.

Fig. 8 shows the same system (i.e., without the ORC) operating during a t.o.p. Again, the power is evenly distributed across the generators during this maneuver [see Fig. 8(a)]. In this case, the maximum voltage drop is 1.57%, corresponding to the propulsion system bus [see Fig. 8(b)]. It can be observed that the voltage drop increases linearly with power demand. The reference and measured speeds for the propulsion system and the mechanical torques of the generators are shown in Fig. 8(c).

From these results, it can be concluded that the power sharing between generators is appropriate. Regarding voltages, the dc voltages of all the buses are within permissible limits as a consequence of an adequate sizing of the sections of the conductors that results in low voltage drops. However, it should be noted that the voltages of the different buses are not controlled and depend on the power demanded by the loads. Hence, if the power demand increases, the voltage drops of the buses will also increase, potentially to the point where the limits could be exceeded.

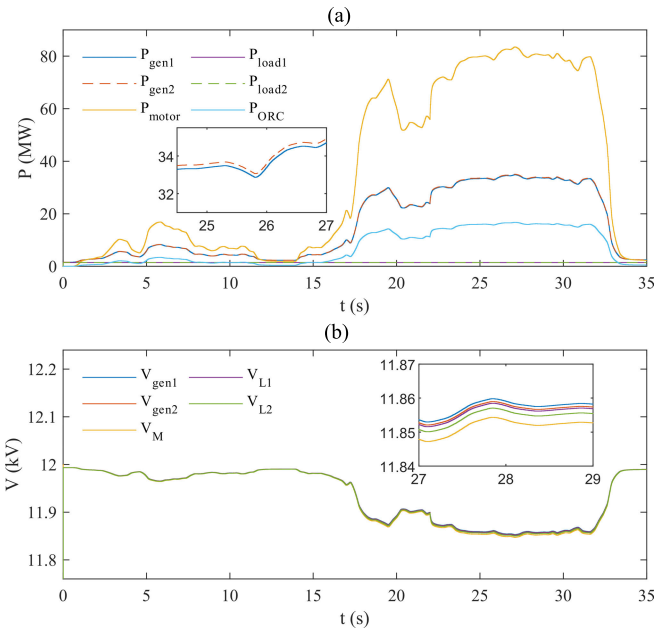

Fig. 9. Case study I, t.o.p. scenario w/ ORC. (a) Power and (b) voltage.

The operation of the system with an integrated ORC was then analyzed during s.s.r.m. and t.o.p. As shown in Fig. 1, the ORC system is connected to the same bus as generator 1. Fig. 9 shows the same system in case study I, with the addition of an ORC system, operating during a t.o.p. The power generated by the ORC system results in a reduction in the power produced by the generators, which is evenly distributed across them both [see Fig. 9(a)]. In this scenario, the maximum voltage drop, corresponding to the propulsion system bus, is 1.27% [see Fig. 9(b)]. The improvement represented by this voltage drop (0.3% with respect to the scenario without the ORC system) is due to the reduction in power from the generators, which in turn reduces the current flowing through the conductors and hence results in a drop in voltage. It can be concluded from this scenario that the integration of the ORC system in case study I does not affect the performance of the dc network, and since the generators continue to share power equally, the system still lacks control of the voltages, and the profile of the voltages remains effectively the same.

B. Case Study II

In this case study, all the simulations were run according to the paradigm by which each PWM rectifier connected to the generators was controlled so as to keep the dc bus voltage at the fixed reference value of 12 kV.

Fig. 10 shows the operation of the system without ORC during an s.s.r.m. The power from each of the different components is shown in Fig. 10(a). The difference with respect to the same scenario in case study I is that the power from the generators is not evenly distributed. During the first acceleration, both generators share production of the power demanded by the propulsion system. However, once a steady speed is

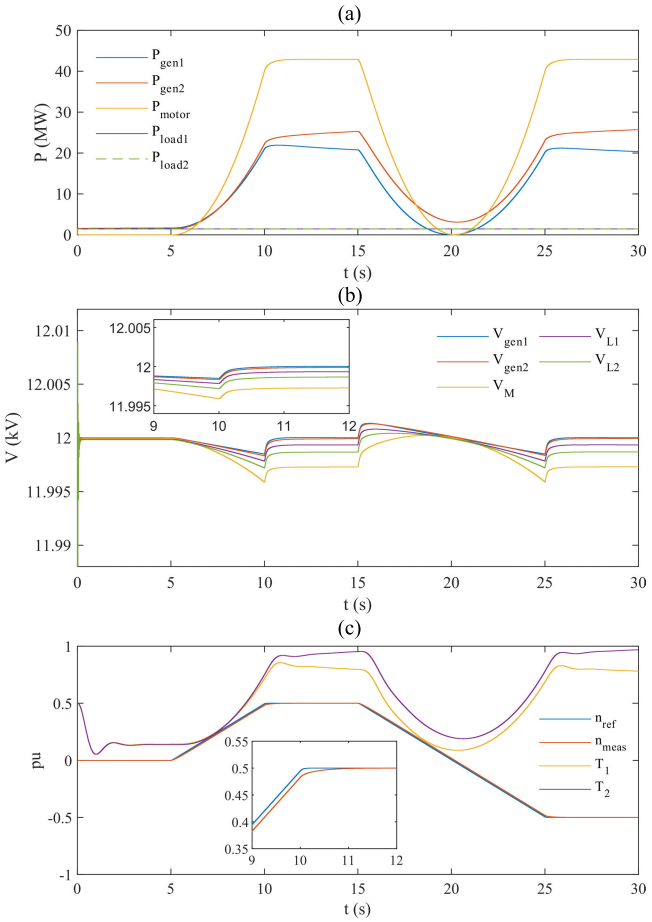

Fig. 10. Case study II, s.s.r.m. scenario w/o ORC. (a) Power, (b) voltage, and (c) propulsion speed and torque of the generators.

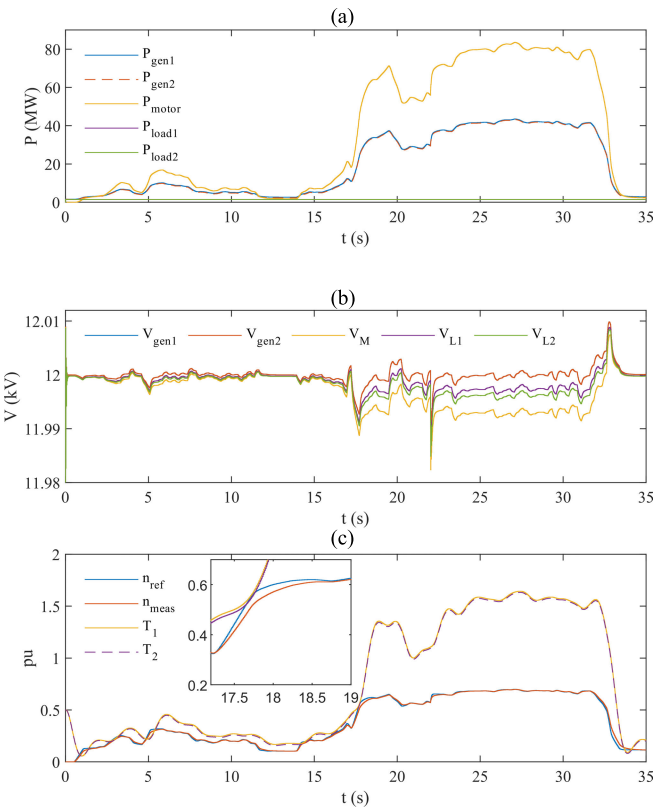

Fig. 11. Case study II, t.o.p. scenario w/o ORC. (a) Power, (b) voltage, and (c) propulsion speed and torque of the generators.

reached, one of the generators raises its power at the same rate as the other reduces it. This new sharing ratio is maintained during the next transitory state and even after the next steady speed is reached. Fig. 10(b) shows the bus voltage when the generators, propulsion system, and loads are connected. It can be observed that the voltage of the different buses remains at around the reference value (12 kV). In this scenario, the voltage drop profile for the different buses is largely flat, with few variations from the reference voltage. The voltage drop is not as large as in the case study I. The maximum voltage drop, which occurs when the demand for propulsion power increases, is 0.04%. The other buses present similar voltage drops, all within the limits imposed by the various standards governing electric ships with dc distribution networks. This is a clear improvement on the results of the previous case study. Furthermore, it can be seen that the voltage levels of the different buses increase during decelerations, even slightly exceeding the reference voltage [at around the 15-s point in Fig. 10(b)]. Fig. 10(c) shows that the propulsion system correctly follows the shaft speed command with a delay of around a second. The differences in mechanical torque in per unit applied to the generator shafts can also be seen.

Fig. 11 shows the results of the same system (i.e., without an ORC) operating during a t.o.p. In this case, the power is evenly distributed across the generators [see Fig. 11(a)], while the voltage of various buses is kept at around the reference value (12 kV). However, it should be highlighted that the voltage drop in the different buses increases linearly with the increase in power demand (see Fig. 11(b) between the 15- and 30-s points). The maximum voltage drop is 0.26% (11.969 kV), corresponding to the propulsion system bus [see Fig. 11(b)]. The reference and measured speeds for the propulsion system and the mechanical torques of the generators are shown in Fig. 11(c). Fig. 11(c) also shows a detail of the slight difference between the mechanical torques of the generators, and one interval in which the delay between the shaft speed command and the measured speed is higher.

In comparison with case study I, replacing the passive rectifiers with controlled rectifiers results in an improved voltage profile for the MVDC network. However, if the integration of an ORC is considered, the system proposed in case study II would not work properly due to the lack of a centralized controller. In case study II, each PWM rectifier is independently controlled to keep the voltage of its bus at a fixed reference value. Considering the scheme shown in Fig. 1, when the ORC system injects current into the bus, the generator connected to that bus reduces its current (i.e., its power) so as to keep the bus voltage at the reference value. Simultaneously, because power generation is shared, the other generator duly increases its power. There is thus a risk that the generators may experience overload or shutdown, making the operation of the electrical network unfeasible.

In both scenarios—s.s.r.m. and t.o.p.—integration of an ORC within the parameters of case study II leads to a

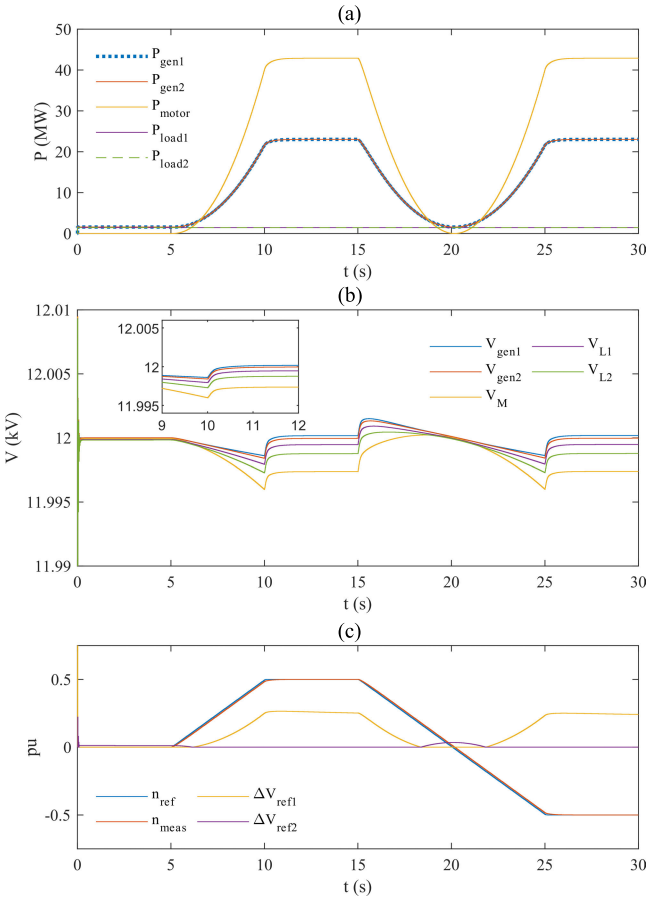

Fig. 12. Case study III, s.s.r.m. scenario w/o ORC. (a) Power, (b) voltage, and (c) propulsion speed and control signals of the centralized control.

shutdown of the generator connected to the bus of the ORC system and an overload of the other generator. The power sharing between the generators is highly dependent on the bus to which the ORC system is connected. Such imbalances may not always result, but the configuration in case study II is nevertheless unreliable and hence unsuitable for ORC integration.

C. Case Study III

In this case study, the simulations were carried out with the configuration by which the reference values for the control loops of each PWM rectifier were sent by the centralized control described in Section III-B.

Fig. 12 shows the operation of this configuration during an s.s.r.m. without an ORC system. It can be seen that the results are fairly similar to those in Fig. 10, with the following differences. The power is evenly distributed across the generators during this maneuver [see Fig. 12(a)]. The simulation results in slight differences between the voltage drops, the maximum of which is 0.04%, corresponding to the bus to which the propulsion system is connected [see Fig. 12(b)]. The equal distribution of power is due to the control signals ΔV_{ref1} and ΔV_{ref2} sent by the centralized controller, acting mainly on the centralized controller voltage control loop for generator 1 [see Fig. 12(c)]. In the case of the control loop for generator 2, it acts during the change in direction of the shaft rotation.

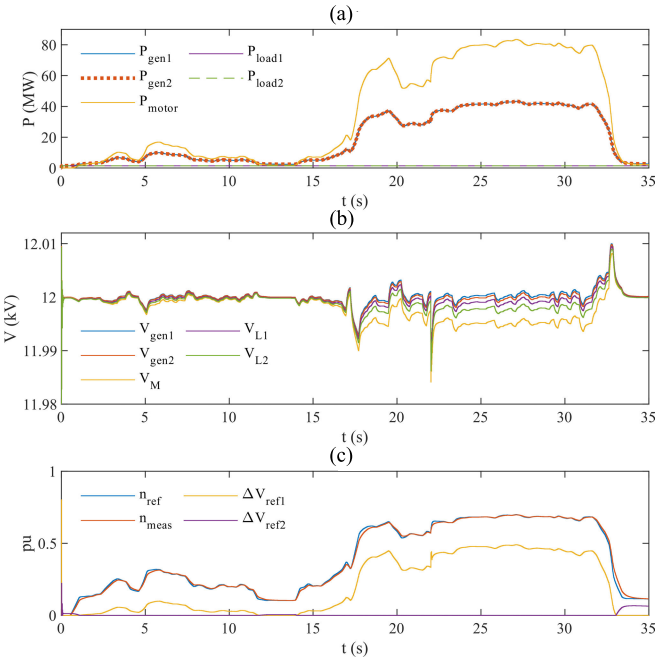

Fig. 13. Case study III, t.o.p. scenario w/o ORC. (a) Power, (b) voltage, and (c) propulsion speed and control signals of the centralized control.

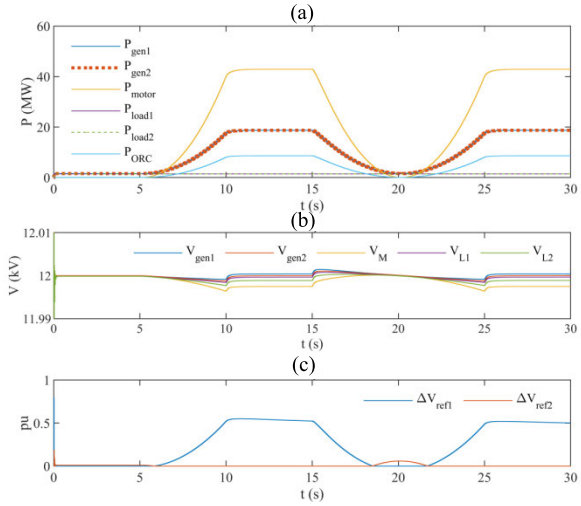

Fig. 14. Case study III, s.s.r.m. scenario w/ ORC. (a) Power, (b) voltage, and (c) control signals of the centralized control.

Fig. 13 shows the same system in operation during a t.o.p. Again, the results are rather similar to those of the analogous scenario in case study II (see Fig. 11). However, in this instance, the power is evenly distributed across the generators during this maneuver [see Fig. 13(a)]. The voltage profile [see Fig. 13(b)] is also similar to that of case study II. Fig. 13(c) shows that for most of the time, the centralized controller acts on the voltage control loop of generator 1 (ΔV_{ref1}), and it is only at the end of the simulation that it stops acting on it and starts acting on the control loop of generator 2 (ΔV_{ref2}).

The simulations were also carried out for the two scenarios of s.s.r.m. and t.o.p. with the incorporation of the ORC system. Fig. 14 shows the system configuration for case study III operating during an s.s.r.m. with the ORC system. In Fig. 14(a), it can be seen that the power is evenly distributed

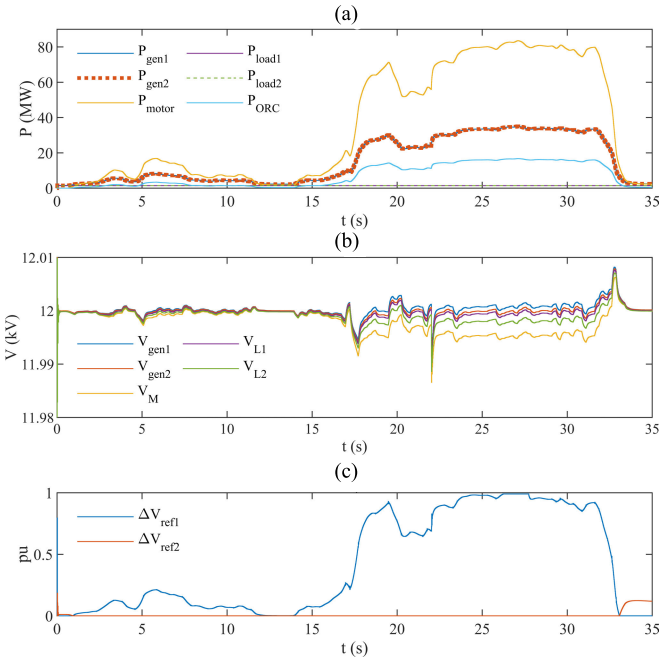

Fig. 15. Case study III, t.o.p. scenario w/ ORC. (a) Power, (b) voltage, and (c) control signals of the centralized control.

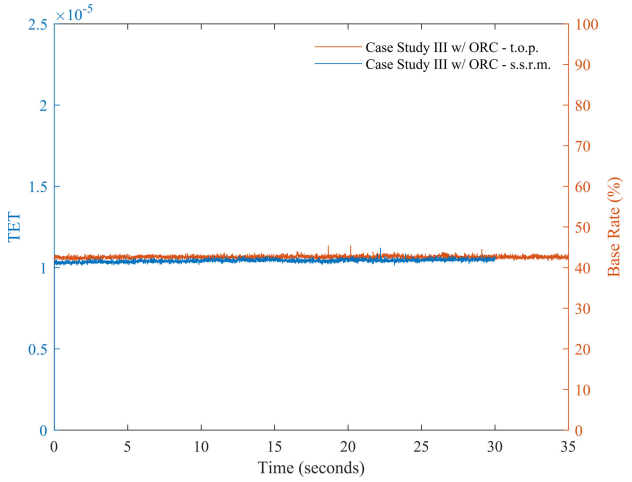

Fig. 16. TETs in case study III: real-time simulations of scenarios w/ ORC running on target computer.

across the generators during this maneuver. The voltage drop in various buses presents an almost flat profile with hardly any variations from the reference voltage [see Fig. 14(b)], similar to the scenario when the ORC system was not connected. Fig. 14(c) shows the control signals ΔV_{ref1} and ΔV_{ref2} sent by the centralized controller, which facilitate both the balanced power sharing between generators and the injection of power from the ORC system. The successful integration of the ORC system is confirmed by the results of the ship operating under the t.o.p. shown in Fig. 15.

From these scenarios and the earlier outcomes of case study II, it can be inferred that a global controller is essential for the integration of the ORC system.

In addition, the real-time performance of the simulations in this case study with the ORC system connected is shown in Fig. 16. It shows the task execution time (TET) for the s.s.r.m. and t.o.p. scenarios. TET, represented on the left-hand vertical axis, is an average of the measured CPU times, in seconds, to run the model equations and post outputs during each sample interval. As can be observed, the TET for both simulations is around 10 μs. Given that the base sample rate is 25 μs, the target computer CPU (speedgoat performance real-time target machine) needed about 40% of the sample time to complete the real-time activities (see the right-hand vertical axis).

V. Discussion

The proposed system was studied using a paradigm designed with the objective of allowing real-time simulations. The main actors in the control of the electrical networks are the power converters of the generators. Apart from these, the main disturbances affecting the network operation are the propulsion system and the ORC system. The power converters of the generators and propulsion system were modeled using average-value power converters composed of a controlled current source and a controlled voltage source, whose control input is the duty cycle. Regarding the power converter modeling techniques, these can be classified into five groups according to the level of detail of the models: switching devices (modeled by IGBTs/diodes controlled by firing pulses produced by a PWM generator); switching function (modeled by a switching function controlled by firing pulses produced by a PWM generator); switching function with PWM averaging (similar to the previous group, except that the firing pulses produced by the PWM generator are replaced by pulse averaging); switching function controlled by the reference voltage (a PWM generator is not required); and a controlled voltage source (whose voltage is the reference voltage). The first of these is the most accurate, while the fifth is the fastest for simulations, although its accuracy is very low. Only the techniques from 3 to 5 allow real-time simulations. This work used the third approach, as it was the most suitable for the objectives. Nevertheless, in terms of accuracy, it remains pending for future works to study the behavior of the interaction between the generators and the dc network using more detailed modeling techniques and shorter simulations that only consider specific transitory scenarios. In this respect, one area worthy of further study is the performance of the PWM rectifiers, in addition to the detailed waveforms of current/voltages and the effect of different patterns on the PWM generation (e.g., for harmonic analysis).

Real-time model execution is crucial for future research since it makes it possible to test centralized control strategies using controller hardware-in-the-loop (C-HIL) and to test the integration of the ORC using power hardware-in-the-loop (P-HIL). In the case of the former, the centralized control would be implemented via a hardware controller (e.g., microcontroller card). This controller would be connected to a real-time machine (e.g., speedgoat performance real-time target machine) loaded with the model of the ship. In this way, the controller being tested would not be able to distinguish whether it is controlling the real ship or a real-time simulation—it would receive measurements from the real-time

machine and respond with control signals. In the case of the latter, the model of the ORC system could be replaced by a lab-scale ORC system connected to the target machine to test its integration experimentally.

It should be emphasized once more that the model that served as the basis to develop the paradigm described in this work is freely accessible for download [8], allowing other researchers to continue this line of research and contribute to its advancement.

The findings of this discussion suggest directions for further research. On the one hand, there is ample scope to develop new centralized controls for MVDC electric propulsion ships with WHRSs based on optimization methods (such as dynamic/linear programming, evolutionary algorithms, etc.). On the other hand, there are various avenues to be explored for energy storage systems aimed at improving the voltage drop profile of the network (whether batteries or ultracapacitors, or even both). There is also the question of how these should be integrated into the centralized control and how to best place them in the network buses.

Other future work focused on the thermal aspect of the WHRS, i.e., on the optimization of the ORC working fluid or even other cycles such as Kalina, remains pending as this work has focused solely on the integration of the WHRS from an electrical point of view. Accordingly, it makes sense to conduct some research into the quantification of the efficiency improvement (e.g., in terms of overall used fuel).

VI. Conclusion

This work proposes a measure for reducing maritime transport emissions. The measure was formulated as a paradigm resulting from the systematic literature review described in Section II, which concluded that: 1) ORC technology is the best choice for large tonnage ships; 2) using electric propulsion increases the capacity to reuse the energy produced by the ORC; and 3) using dc networks ease the integration of the ORC. Based on these conclusions, the study defines a paradigm for electric propulsion in ships composed of VSC-MT MVDC networks and ORC acting as WHRS. In addition, it was found that ORC integration depends on properly controlling the VSC-MT MVDC network so as to successfully manage the tradeoff between voltage regulation and power sharing.

The results of real-time simulations for testing the integration of the ORC system in the ship MVDC network enabled some conclusions to be drawn. Although the integration of the ORC system is simplified for dc networks in comparison to ac networks (mainly because synchronization of paralleled generators is unnecessary), the integration of the ORC is not a trivial problem. The results of the simulations showed that an appropriate design of the dc network topology and control system is required for the correct performance of the ship under any scenario. It was concluded that replacing the passive rectifiers with controlled rectifiers improved the voltage profile of the MVDC network. Furthermore, it was inferred that the design of the global controller is an essential element in the integration of the ORC system. Although the focus of this work is on the ORC, the proposed solution could also be used to integrate other types of WHRSs that produce electrical energy via generators.

References

[1] (2021). *International Shipping*. International Energy Agency (IEA), Paris, France. [Online]. Available: https://www.iea.org/reports/international-shipping

[2] Climate Watch. *Historical GHG Emissions*. Accessed: May 2, 2023. [Online]. Available: https://www.climatewatchdata.org/ghg-emissions

[3] M. Okubo and T. Kuwahara, "Chapter 1—Introduction," in *New Technologies for Emission Control in Marine Diesel Engines*. London, U.K.: Butterworth-Heinemann, 2020, ch. 1, pp. 1–24, doi: 10.1016/B978-0-12-812307-2.00001-8.

[4] V. Eyring, H. W. Köhler, A. Lauer, and B. Lemper, "Emissions from international shipping: 2. Impact of future technologies on scenarios until 2050," *J. Geophys. Res., Atmos.*, vol. 110, no. 17, p. 2, Sep. 2005, doi: 10.1029/2004jd005620.

[5] S. Lion, I. Vlaskos, and R. Taccani, "A review of emissions reduction technologies for low and medium speed marine diesel engines and their potential for waste heat recovery," *Energy Convers. Manage.*, vol. 207, Mar. 2020, Art. no. 112553, doi: 10.1016/j.enconman.2020.112553.

[6] D. V. Singh and E. Pedersen, "A review of waste heat recovery technologies for maritime applications," *Energy Convers. Manage.*, vol. 111, pp. 315–328, Mar. 2016, doi: 10.1016/j.enconman.2015.12.073.

[7] C. Nuchturee, T. Li, and H. Xia, "Energy efficiency of integrated electric propulsion for ships—A review," *Renew. Sustain. Energy Rev.*, vol. 134, Dec. 2020, Art. no. 110145, doi: 10.1016/j.rser.2020.110145.

[8] G. Dudgeon. (2021). *Electric Ship Model in Simscape*. MathWorks. [Online]. Available: https://github.com/mathworks/Two-Zone-MVDC-Electric-Ship

[9] G. Sulligoi, A. Vicenzutti, and R. Menis, "All-electric ship design: From electrical propulsion to integrated electrical and electronic power systems," *IEEE Trans. Transport. Electrific.*, vol. 2, no. 4, pp. 507–521, Dec. 2016, doi: 10.1109/TTE.2016.2598078.

[10] J. Hou, J. Sun, and H. F. Hofmann, "Mitigating power fluctuations in electric ship propulsion with hybrid energy storage system: Design and analysis," *IEEE J. Ocean. Eng.*, vol. 43, no. 1, pp. 93–107, Jan. 2018, doi: 10.1109/JOE.2017.2674878.

[11] J. Hou, Z. Song, H. Park, H. Hofmann, and J. Sun, "Implementation and evaluation of real-time model predictive control for load fluctuations mitigation in all-electric ship propulsion systems," *Appl. Energy*, vol. 230, pp. 62–77, Nov. 2018, doi: 10.1016/j.apenergy.2018.08.079.

[12] J. Hou, J. Sun, and H. Hofmann, "Control development and performance evaluation for battery/flywheel hybrid energy storage solutions to mitigate load fluctuations in all-electric ship propulsion systems," *Appl. Energy*, vol. 212, pp. 919–930, Feb. 2018, doi: 10.1016/j.apenergy.2017.12.098.

[13] F. D'Agostino, D. Kaza, M. Martelli, G.-P. Schiapparelli, F. Silvestro, and C. Soldano, "Development of a multiphysics real-time simulator for model-based design of a DC shipboard microgrid," *Energies*, vol. 13, no. 14, p. 3580, Jul. 2020, doi: 10.3390/en13143580.

[14] J. N. Forestieri and M. Farasat, "Energy flow control and sizing of a hybrid battery/supercapacitor storage in MVDC shipboard power systems," *IET Electr. Syst. Transp.*, vol. 10, no. 3, pp. 275–284, Sep. 2020, doi: 10.1049/iet-est.2019.0161.

[15] K. Kuiken, *Diesel Engines*, 3rd ed. Onnen, The Netherlands: Target Global Energy Training, 2017.

[16] Fujian Opcon Energy Technology Co. *OPCON Powerbox ORC-Series*. Accessed: Jul. 13, 2023. [Online]. Available: http://www.fj-opcon.com/en/Product/detail/id/2

[17] R. D. Geertsma, R. R. Negenborn, K. Visser, and J. J. Hopman, "Design and control of hybrid power and propulsion systems for smart ships: A review of developments," *Appl. Energy*, vol. 194, pp. 30–54, May 2017, doi: 10.1016/j.apenergy.2017.02.060.

[18] M. R. Patel, *Shipboard Propulsion, Power Electronics, and Ocean Energy*. Boca Raton, FL, USA: CRC Press, 2017.

[19] N. Doerry, "Naval power systems: Integrated power systems for the continuity of the electrical power supply," *IEEE Electrific. Mag.*, vol. 3, no. 2, pp. 12–21, Jun. 2015, doi: 10.1109/MELE.2015.2413434.

[20] E. Skjong, R. Volden, E. Rødskar, M. Molinas, T. A. Johansen, and J. Cunningham, "Past, present, and future challenges of the marine vessel's electrical power system," *IEEE Trans. Transport. Electrific.*, vol. 2, no. 4, pp. 522–537, Dec. 2016, doi: 10.1109/TTE.2016.2552720.

[21] F. D. Kanellos, G. J. Tsekouras, and J. Prousalidis, "Onboard DC grid employing smart grid technology: Challenges, state of the art and future prospects," *IET Electr. Syst. Transp.*, vol. 5, no. 1, pp. 1–11, Mar. 2015, doi: 10.1049/iet-est.2013.0056.

[22] Y. Yuan, J. Wang, X. Yan, B. Shen, and T. Long, "A review of multi-energy hybrid power system for ships," *Renew. Sustain. Energy Rev.*, vol. 132, Oct. 2020, Art. no. 110081.

[23] S. Castellan, R. Menis, A. Tessarolo, F. Luise, and T. Mazzuca, "A review of power electronics equipment for all-electric ship MVDC power systems," *Int. J. Electr. Power Energy Syst.*, vol. 96, pp. 306–323, Mar. 2018.

[24] Z. Wang, J. He, Y. Xu, and F. Zhang, "Distributed control of VSC-MTDC systems considering tradeoff between voltage regulation and power sharing," *IEEE Trans. Power Syst.*, vol. 35, no. 3, pp. 1812–1821, May 2020, doi: 10.1109/TPWRS.2019.2953044.

[25] J. Rodriguez, S. Bernet, B. Wu, J. O. Pontt, and S. Kouro, "Multilevel voltage-source-converter topologies for industrial medium-voltage drives," *IEEE Trans. Ind. Electron.*, vol. 54, no. 6, pp. 2930–2945, Dec. 2007, doi: 10.1109/TIE.2007.907044.

[26] M. H. Rashid, "Force-commutated three-phase controlled rectifiers," in *Power Electronics Handbook*. St. Louis, MO, USA: Elsevier, 2017.

[27] K. Rouzbehi, A. Miranian, J. I. Candela, A. Luna, and P. Rodriguez, "A generalized voltage droop strategy for control of multiterminal DC grids," *IEEE Trans. Ind. Appl.*, vol. 51, no. 1, pp. 607–618, Jan. 2015, doi: 10.1109/TIA.2014.2332814.

[28] U. Javaid, F. D. Freijedo, D. Dujic, and W. van der Merwe, "Dynamic assessment of source—Load interactions in marine MVDC distribution," *IEEE Trans. Ind. Electron.*, vol. 64, no. 6, pp. 4372–4381, Jun. 2017, doi: 10.1109/TIE.2017.2674597.

[29] U. Javaid, F. D. Freijedo, W. van der Merwe, and D. Dujic, "Stability analysis of multi-port MVDC distribution networks for all-electric ships," *IEEE J. Emerg. Sel. Topics Power Electron.*, vol. 8, no. 2, pp. 1164–1177, Jun. 2020.

[30] D. Paul, "A history of electric ship propulsion systems," *IEEE Ind. Appl. Mag.*, vol. 26, no. 6, pp. 9–19, Nov. 2020, doi: 10.1109/MIAS.2020.3014837.

[31] C.-L. Su, K.-L. Lin, and C.-J. Chen, "Power flow and generator-converter schemes studies in ship MVDC distribution systems," *IEEE Trans. Ind. Appl.*, vol. 52, no. 1, pp. 50–59, Jan. 2016, doi: 10.1109/TIA.2015.2463795.

[32] Z. Jin, L. Meng, J. M. Guerrero, and R. Han, "Hierarchical control design for a shipboard power system with DC distribution and energy storage aboard future more-electric ships," *IEEE Trans. Ind. Informat.*, vol. 14, no. 2, pp. 703–714, Feb. 2018, doi: 10.1109/TII.2017.2772343.

[33] N. Doerry and J. Amy, "MVDC shipboard power system considerations for electromagnetic railguns," in *Proc. 6th DoD Electromagn. Railgun Workshop*, 2015, pp. 1–8.

[34] *IEEE Recommended Practice for 1 KV To 35 KV Medium-Voltage DC Power Systems on Ships*, IEEE Standard 1709-2018, Revision of IEEE Standard 1709-2010, 2018, pp. 1–54, doi: 10.1109/IEEESTD.2018.8569023.

[35] M. M. Islam, *Handbook To IEEE Standard 45: A Guide To Electrical Installations on Shipboard*. Hoboken, NJ, USA: Wiley, 2004, p. 394, doi: 10.1002/9781118098844.ch7.

[36] Naval Sea Systems Command. (2019). *Naval Power and Energy Systems Technology Development Roadmap*. [Online]. Available: https://www.navsea.navy.mil/Resources/NPES-Tech-Development-Roadmap/

[37] *IEEE Standard for Power Electronics Open System Interfaces in Zonal Electrical Distribution Systems Rated Above 100 KW*, IEEE Standard 1826-2020, Revision of IEEE Standard 1826-2012, 2020, pp. 1–44, doi: 10.1109/IEEESTD.2020.9271958.

[38] A. K. Ådnanes, *Maritime Electrical Installations and Diesel Electric Propulsion*. Zürich, Switzerland: ABB, 2003. [Online]. Available: https://books.google.es/books?id=E0q-oAEACAAJ

[39] E. P. Wiechmann, P. Aqueveque, R. Burgos, and J. Rodriguez, "On the efficiency of voltage source and current source inverters for high-power drives," *IEEE Trans. Ind. Electron.*, vol. 55, no. 4, pp. 1771–1782, Apr. 2008, doi: 10.1109/TIE.2008.918625.

[40] Wärtsilä Webpage. (2019). *Wärtsilä 46F Product Guide*. Accessed: May 7, 2023. [Online]. Available: https://go.wartsila.com/l/251562/2022-06-15/2v95qyq?MP_Content_Center=MP-Product-guide-W46F

[41] Honeywell Refrigerants Webpage. *Solstice® zd (R-1233zd) Guidelines*. Accessed: May 7, 2023. [Online]. Available: https://www.honeywell-refrigerants.com/europe/wp-content/uploads/2015/08/Solstice-zd-Handling-Guidelines.pdf

[42] J. W. Dixon, *Handbook of Power Electronics*. New York, NY, USA: Academic, 2001, pp. 599–627.

[43] F. Baldi, F. Ahlgren, T.-V. Nguyen, M. Thern, and K. Andersson, "Energy and exergy analysis of a cruise ship," *Energies*, vol. 11, no. 10, p. 2508, Sep. 2018, doi: 10.3390/en11102508.

[44] *IEEE Recommended Practice for Electrical Installations on Shipboard-Electrical Testing*, IEEE Standard 45.6-2016, 2017, pp. 1–39, doi: 10.1109/IEEESTD.2017.7865875.

Juan P. Torreglosa was born in Seville, Spain, in 1985. He received the M.Sc. degree in industrial engineering and the Ph.D. degree from the University of Jaén, Linares, Spain, in 2009 and 2012, respectively.

His experience as a Researcher began when he worked on various projects at the University of Jaén from 2009 to 2015. He has been an Associate Professor at the Department of Electrical Engineering, University of Huelva, Huelva, Spain, since 2015. His current research interests include the integration of renewable energy sources, dc network applications, transport electrification, and energy management systems.

David Vera Candeas received the Ph.D. degree in industrial engineering from the University of Jaén, Linares, Spain, in 2013.

He has been a Teacher and a Researcher at the Department of Electric Engineering, University of Jaén, since 2008. He has been involved in research projects for the Spanish Ministry of Science and Education and the European Commission. His research interests include biomass energy, distributed generation technologies, climatic change, and energy economy.

Diego A. López García received the Ph.D. degree in automats and systems engineering from the University of Huelva, Huelva, Spain, in 2011.

He has been an Industrial Engineer at the University of Seville, Seville, Spain, specializing in electronics, since 2000. From 2000 to 2003, was a Project Manager at Landata Payma S.A., devoted to telecommunication infrastructures and networks. Since 2003, he has been a Professor at the Department of Electronic Engineering, Computer Systems and Automatics, University of Huelva. In addition, he participated in around ten teaching innovation projects related to remote laboratories and ICTs applied to the learning process. He has published more than 20 articles taking into account journals and congresses. His research interests include network security (e-voting), robotics (motion planning), and smart grids.

Alejandro Pérez Vallés was born in Arahal, Seville, Spain. He received the Ind.Eng. degree from the University of Cádiz, Cádiz, Spain, in 2007, and the Ph.D. degree from the School of Engineering, University of Huelva, Huelva, Spain, in 2020.

He is currently the Head of the Department of Electrical Engineering and Thermal, Design and Projects, University of Huelva, where he has been an Associate Professor since 1999. He is also a Researcher at the Huelva Scientific and Technological Center (CCTH) and a member of the research group Electrical and Electronics of La Rábida, GEYER. His research interests include electric power quality, design, and control of active power conditioners, with emphasis on the analysis and measurement of the quality of electrical power under conditions of asymmetry and distortion. Finally, he has participated in different research projects funded through competitive calls.

José Antonio Hernández-Torres was born in Huelva, Spain, in 1995. He received the B.Sc. degree in mechanical engineering and the M.Sc. degree in industrial engineering from the University of Huelva, Huelva, in 2017 and 2019, respectively, where he currently pursuing the Ph.D. degree.

He is also a Teaching Assistant at the University of Huelva. His research interests include renewable energy systems, power generation machinery, and energy management systems.

Jesus Clavijo-Camacho received the B.E.E. degree and the master's degree in industrial engineering from the University of Huelva, Huelva, Spain, in 2021 and 2023, respectively, where he is currently pursuing the Ph.D. degree.

He is a part-time Lecturer at Huelva University. His research interests include microgrids as a key piece for renewable energy penetration and electric distribution system improvement.